Toxicology 313 (2013) 59–69

Contents lists available at ScienceDirect

Toxicology

journal homepage: www.elsevier.com/locate/toxicol

Cell membrane damage and protein interaction induced by copper containing nanoparticles—Importance of the metal release process

Hanna L. Karlsson[a,*], Pontus Cronholm[b], Yolanda Hedberg[c], Malin Tornberg[d], Laura De Battice[e], Sofia Svedhem[e], Inger Odnevall Wallinder[c]

[a] Division of Molecular Toxicology, Institute of Environmental Medicine, Karolinska Institutet, Stockholm, Sweden
[b] Unit for Analytical Toxicology, Department of Biosciences and Nutrition, Karolinska Institutet, Stockholm, Sweden
[c] KTH Royal Institute of Technology, Division of Surface and Corrosion Science, Department of Chemistry, Stockholm, Sweden
[d] Swerea KIMAB AB, Box 55970, 102 16 Stockholm, Sweden
[e] Department of Applied Physics, Chalmers University of Technology, 412 96, Göteborg, Sweden

ARTICLE INFO

Article history:
Received 9 November 2012
Received in revised form 14 February 2013
Accepted 17 July 2013
Available online 26 July 2013

Keywords:
Nanoparticles
Toxicity
Copper
Cell membrane
Hemoglobin
Metal release

ABSTRACT

Cu-containing nanoparticles are used in various applications in order to *e.g.* achieve antimicrobial activities and to increase the conductivity of fluids and polymers. Several studies have reported on toxic effects of such particles but the mechanisms are not completely clear. The aim of this study was to investigate the interactions between cell membranes and well-characterized nanoparticles of CuO, Cu metal, a binary Cu-Zn alloy and micron-sized Cu metal particles. This was conducted *via in vitro* investigations of the effects of the nanoparticles on (*i*) cell membrane damage on lung epithelial cells (A549), (*ii*) membrane rupture of red blood cells (hemolysis), complemented by (*iii*) nanoparticle interaction studies with a model lipid membrane using quartz crystal microbalance with dissipation monitoring (QCM-D). The results revealed that nanoparticles of the Cu metal and the Cu-Zn alloy were both highly membrane damaging and caused a rapid (within 1 h) increase in membrane damage at a particle mass dose of 20 μg/mL, whereas the CuO nanoparticles and the micron-sized Cu metal particles showed no such effect. At similar nanoparticle surface area doses, the nano and micron-sized Cu particles showed more similar effects. The commonly used LDH (lactate dehydrogenase) assay for analysis of membrane damage was found impossible to use due to nanoparticle-assay interactions. None of the particles induced any hemolytic effects on red blood cells when investigated up to high particle concentrations (1 mg/mL). However, both Cu and Cu-Zn nanoparticles caused hemoglobin aggregation/precipitation, a process that would conceal a possible hemolytic effect. Studies on interactions between the nanoparticles and a model membrane using QCM-D indicated a small difference between the investigated particles. Results of this study suggest that the observed membrane damage is caused by the metal release process at the cell membrane surface and highlight differences in reactivity between metallic nanoparticles of Cu and Cu-Zn and nanoparticles of CuO.

1. Introduction

Copper (Cu) is an essential trace element in living organisms that plays a vital role in the function of proteins. However, since copper is redox-active, its transport into cells is tightly controlled. The rapidly emerging use of nanoparticles on the global market has resulted in an increased number of applications for Cu and CuO nanoparticles in various products. The reason is primarily related to their antimicrobial activities (Ren et al., 2009), for example taken into account in textiles (Torres et al., 2010) and in dental applications to prevent infections (Allaker, 2010). In both examples, their use poses an immediate risk for human exposure. Cu nanoparticles are furthermore used to make *e.g.* fluids and polymers conductive (Saterlie et al., 2011; Pham et al., 2012) and have been suggested to replace silver and gold in ink-jet printable electronics (Luechinger et al., 2008). Chemical, physical and functional properties of nanometer sized particles often differ compared with

Abbreviations: DLS, dynamic light scattering; QCM-D, quartz crystal microbalance with dissipation monitoring; DMEM, Dulbecco's Modified Eagle's medium; AAS, atomic absorption spectroscopy; TEM, transmission electron microscopy; EELS, electron energy-loss spectrometry; STEM, scanning transmission electron microscopy; EDS, energy dispersive spectroscopy; XRD, X-ray diffraction; XPS, X-ray photoelectron spectroscopy; PCCS, Photon Cross Correlation Spectroscopy; LDH, Lactate dehydrogenase; INT, iodonitrotetrazolium; POPC, 1-palmitoyl-2-oleoyl-sn-glycero-3-phosphocholine; POPS, 1-palmitoyl-2-oleoyl-sn-glycero-3-phospho-L-serine; POPG, 1-hexadecanoyl-2-(9Z-octadecenoyl)-sn-glycero-3-phospho-(1'-rac-glycerol).

* Corresponding author at: Division of Molecular Toxicology, Institute of Environmental Medicine, Nobels väg 13, Karolinska Institutet, 171 77 Stockholm, Sweden. Tel.: +46 8 524 875 76.
E-mail address: Hanna.L.Karlsson@ki.se (H.L. Karlsson).

0300-483X
http://dx.doi.org/10.1016/j.tox.2013.07.012

particles of larger size or dissolved species of the same element (Roduner, 2006). These unusual properties can also render the particles toxic to cells and organisms. Results from *in vitro* studies comparing the toxicity of various metal-containing nanoparticles have shown copper-containing nanoparticles to be more toxic when compared with other nanoparticles (Karlsson et al., 2008; Lanone et al., 2009; Sun et al., 2012). For example Lanone et al. (2009) compared the toxicity of 24 manufactured nanoparticles in the human lung cell line A549 as well as in a macrophage cell line (THP-1). Nanoparticles of copper (Cu, CuO) and ZnO were found most toxic with IC50 values of 5–10 μg/mL for THP-1 cells and somewhat higher (typically 10–50 μg/mL) for A549 cells. Nanoparticles of CuO have furthermore shown higher toxicity compared with micron-sized particles of CuO in human lung cells (Karlsson et al., 2009; Wang et al., 2012), in microorganisms (Gunawan et al., 2011) and in yeast cells (Kasemets et al., 2009). Size dependent effects have also been observed in animal studies, *i.e.* Cu nanoparticles were reported more toxic compared with micron-sized Cu particles following oral administration to rats (Chen et al., 2006).

Nanoparticles tend to release a higher amount of metal ions and dissolve faster in a given solution volume compared with larger-sized particles. An important question is thus whether the observed toxicity solely can be explained by released metal ions/ionic species, or whether some effects actually are particle-related, *i.e.* depend on cellular mechanisms at the nano-scale. Previous studies have shown that the presence of the solid particles is important for the toxic response observed. Less toxicity was for example observed when cultured cells were exposed to the same mass dose of Cu from a soluble Cu-compound, or to the released fraction of ionic Cu (*i.e.* the ionic species released to the cell media) when compared with the same mass dose of Cu from nanoparticles of Cu or CuO (Karlsson et al., 2008; Midander et al., 2009). Similar findings were recently also observed in a study using the same lung cell line (A549) in which it was concluded that dissolved Cu ions contributed to less than 50% of the overall cytotoxicity induced by CuO nanoparticles (Wang et al., 2012). A likely reason is that the presence of the solid particles increases the cellular uptake *via* endocytotic mechanisms and that Cu ionic species subsequently are released within the cells, a process often referred to as "the Trojan horse mechanism" (Studer et al., 2010; Wang et al., 2012; Cronholm et al., 2013). Copper ions are redox active, which means that the high intracellular concentration gained after dissolution of CuO nanoparticles within the cell likely results in massive oxidative stress. Various signs of oxidative stress and genotoxicity have been observed upon cellular exposure to CuO nanoparticles. These signs include the induction of catalase and superoxide dismutase, the formation of intracellular ROS and oxidative DNA lesions as well as up-regulation of genes responding to oxidative stress and genotoxicity (Karlsson et al., 2008; Ahamed et al., 2010; Hanagata et al., 2011).

Previous studies by the authors indicate that nanoparticles of CuO and Cu may exert toxicity *via* different mechanisms following cell exposure. Whereas nanoparticles of CuO become endocytosed by the cells within the first hours of contact with subsequent DNA damage, Cu nanoparticles appear to target the cell membrane with a rapid loss of membrane integrity and cell death (Karlsson et al., 2008; Midander et al., 2009). The present study further investigates these different mechanisms with a focus on the interaction between the cell membrane and different Cu-based particles including nano- and micron sized copper metal particles (Cu nano and Cu micro), a nano-sized binary copper-zinc alloy (Cu-Zn nano) and copper oxide nanoparticles (CuO nano). The reason for including the Cu-Zn alloy with 40% Zn is its susceptibility for dezincification, a process where zinc preferentially is dissolved *via* corrosion processes in aqueous systems leaving a porous copper-rich structure behind (Marshakov, 2002; Selvaraj et al., 2003). A comparison of the toxic response of the different Cu-based particles enables a possibility to gain insight in the mechanisms for toxicity and furthermore in the possibilities for grouping metals and alloys to enable read-across for risk- and hazard assessment and management. The benefit of such an approach is a reduced need for animal testing of a vast amount of metal-based nanoparticles present and to be developed for different applications on the market. Another essential question to address is whether it is possible to predict nanoparticle toxicity based on toxicity data generated for larger micron-sized particles as possibly some effects are nano-specific.

Here, Cu nanoparticle induced cell membrane damage was investigated *in vitro* following exposure of lung epithelial cells (A549) and membrane rupture of red blood cells (hemolysis). The hemolytic assay has previously been used in various studies investigating membrane damage caused by *e.g.* SiO_2 nanoparticles (Lin and Haynes, 2010; Shi et al., 2012), and is a fast method to analyze particle reactivity with results suggested to correlate fairly well to the inflammatory potential of the particles (Lu et al., 2009). As a final characterization, differences in the particles' properties were investigated in interaction studies using model lipid membranes. Different surface-sensitive techniques can be used in such studies. Here, changes in mass and viscoelastic properties, *e.g.* softness or rigidity of the lipid membrane were investigated by means of quartz crystal microbalance with dissipation monitoring (QCM-D). One important issue for the different methods employed in this study was to identify and elucidate possible nanoparticle-assay interactions.

2. Materials and methods

2.1. Particle characteristics

Previous studies by the authors have investigated the physico-chemical characteristics and the toxicological response of the CuO nanoparticles and the Cu nano- and micron-sized particles of this study (Cronholm et al., 2011; Midander et al., 2009). General particle characteristics are compiled in Table 1. Nanoparticles of the Cu metal and the Cu-40Zn alloy (denoted Cu-Zn) were produced by electrical explosion of copper and brass wires (40 wt.-% Zn and 60 wt.-% Cu), respectively, at Tomsk Polytechnic University, Tomsk, Russia. Detailed information on the production process is given elsewhere (Kwon et al., 2008).

Size distribution measurements of the nanoparticles in supplemented cell medium (composition given in section 2.4) was conducted using dynamic light scattering (DLS), and zeta potential measurements were performed in 1 or 10 mM NaCl using a Zetasizer nano ZS instrument (Malvern, UK). Prior to the measurements, the particles were suspended in supplemented DMEM medium and sonicated in the same manner as for cell exposure (described below). Using the same system, the apparent surface charge (zeta potential) of the particles was analyzed. Particles were suspended in ultrapure water (18.2 MΩ cm) containing 1 mM NaCl and sonicated following the same procedure as described for the cell exposure. The zeta potential was measured by applying an electrical field through the solution causing particles of different charge to migrate at different speed toward the electrodes. DLS and zeta potential measurements were not possible for the micron-sized particles due to sedimentation.

2.2. Metal release

Total concentrations of released copper and zinc into cell media (DMEM) with serum and in saline were analyzed by means of atomic absorption spectroscopy (AAS, Perkin–Elmer AAnalyst 800). Details of the analytical procedure are given elsewhere (Midander et al., 2009). Triplicate samples were prepared for investigations in cell media (5 min and 4 h at 37 °C, 5% CO_2 and saturated humidity, as for the cell exposure) with a particle mass dose of 40 μg/mL and in saline (5 min) at a mass dose of 100 μg/mL, respectively. Measured released metal concentrations are based on at least three replicate readings for each individual sample. Quality assurance tests were performed continuously by analyzing samples of a standard solution every tenth sample. Data is presented as the average value of three independent samples with the blank value (media without any particles) subtracted. The blank value is based on triplicate samples exposed in parallel for each exposure time period and medium.

2.3. Surface properties

Transmission electron microscopy (TEM) investigations were performed using a JEOL JEM 2100F instrument operating at 200k equipped with a CCD-camera and an electron energy-loss spectrometer (EELS). Bright field images and diffraction patterns were recorded in TEM mode. Settings used for high resolution bright field

Table 1
Particle characteristics.

Sample	BET area m^2/g	Primary size (TEM, nm)	Zeta potential (1 mM NaCl)	pH in saline (pH 6.6) after 10 min
Cu mico	0.1		–	–
Cu nano	6.7	100–200	+13.4	7.8
Cu-Zn nano	3.8	50–100	+2.4	8.3
CuO nano	25	20–50	+27.9	6.6

– Not analyzed due to particle sedimentation.

images were a camera length, CL of 2 and an optical length, OL of 3. Elemental analyses were conducted using EELS and energy dispersive spectroscopy, EDS. EELS was performed with settings of $\alpha = 13.2$, $\beta = 20.3$ or 18.4 and a CL of HAADF5 or 8 cm. EELS spectra were recorded for nanoparticles of Cu-Zn and analyses made using the Cu and Zn peaks positioned at 931 and 1020 eV, respectively. EDS analyses were performed in scanning transmission electron microscopy (STEM) mode. TEM copper grids, coated with holy carbon film, were used as support for the nanoparticles. Freshly prepared and sonicated (1 min) particle dispersions in butanol were transferred onto the grids by using pipettes. The solvent evaporated upon air contact. X-ray diffraction (XRD, X'Pert PRO MPD from PANalytical) measurements were conducted to identify crystalline phases. X-ray photoelectron spectroscopy (XPS, Kratos AXIS UltraDLD, Kratos Analytical) measurements were performed to assess the composition of the outermost surface oxide present on the metallic particles using a monochromatic Al X-ray source (150 W). Wide spectra and high resolution spectra (20 eV pass energy) were acquired for the main compositional elements using the carbon (C1s) peak as internal standard. Experimental details are given elsewhere (Midander et al., 2009).

2.4. Trypan blue staining

A549 type II alveolar epithelial cells (obtained from the American Type Culture Collection, ATCC, Manassas, USA) were cultured in DMEM medium (Dulbecco's Minimal Essential Medium, Cat. No. 41965-039, GIBCO® Invitrogen) supplemented with 10% fetal bovine serum, 100 units/mL penicillin, 100 μg/mL streptomycin and 1 mM sodium pyruvate. Trypan blue staining was used to measure cell membrane integrity. Cells were seeded in a 24-well plate approximately 24 h prior to exposure. The particles were suspended in DMEM with serum, vortexed and sonicated for 2*20 s using a probe sonicator. Cells were then exposed to freshly prepared particle doses for given time periods after which the media was removed and the cells washed with 2*0.5 mL PBS. The trypsinated cells were then added to the previously removed exposure media and PBS (possibly containing detached cells). Tubes containing collected exposure media, PBS and trypsinated cells were then centrifuged for 1 min at 6.000 rpm. Finally, all but 400 μL of the supernatant was removed and 30 μL of the remaining cell suspension was stained with trypan blue and incubated for 3 min before counting the percentage of stained cells in a Bürker chamber (approximately 100 to 150 cells were counted for each sample).

2.5. LDH assay interactions

Lactate dehydragenase (LDH) is a stable enzyme, present in all cell types that rapidly is released into the cell culture medium upon damage of the cell membrane. In the assay kit used in the present study (Roche), the released LDH is measured with a coupled enzymatic reaction that results in the conversion of a tetrazolium salt (iodonitrotetrazolium, INT) into formazan (of red color) by diaphorase (see Fig. 4). The LDH activity is determined as NADH oxidation or INT reduction over a defined time period. In order to investigate whether the particles could interact with this assay, particles of different mass dose (10, 20 and 40 μg/mL suspended in saline and sonicated as previously described) were incubated with the reaction mix from the assay kit in a 96-well plate for 15 min after which the absorbance at 490 nm was measured using a microplate spectrophotometer (PowerWave x, Bio-Tek Instruments, Inc., USA). In addition, pure LDH protein (10 units/mL) was mixed with the reaction mix from the assay kit and the absorbance was recorded. The lack of increase of absorbance compared with the control (containing only saline or only LDH in saline, respectively) indicated lack of assay interactions.

2.6. Hemolytic assay and hemoglobin interactions

The procedure for using the hemolytic assay has been described elsewhere (Hedberg et al., 2010). In short, fresh venous blood, from healthy blood donors (Blood Donor Center, KI, Huddinge) was collected in 10 mL EDTA tubes. The samples were gently mixed by inversion, added onto histopaque and centrifuged from which erythrocytes were collected. The cells were washed 3 times with PBS followed by suspension in saline or PBS and subsequently mixed with nanoparticles to a final particle mass dose of 0.5 or 1 mg/mL. 0.1% Trithon was used for total cell lysis. Prior to exposure to the erythrocytes, the particles were suspended in saline (or PBS) to a mass dose of 2 mg/mL, vortexed for 20 s followed by tip sonication (2*20 s) in order to reduce particle agglomeration. All exposures were conducted at dark conditions on a shaking table for 30 min (samples briefly mixed every 10 min). Following incubation, the erythrocyte-particle suspensions were centrifuged for 5 min at 10,000 rpm (15 °C). Hemoglobin levels of the supernatant were determined *via* optical density (absorbance) measurements, a measure of lysed erythrocytes, by using a microplate scanning spectrophotometer (PowerWave x, Bio-Tek Instruments, Inc., USA) at 540 nm (reference 620 nm) in two separate wells of the well plate. Three independent experiments were conducted for each particle type. For hemoglobin interactions, human hemoglobin A0 (Sigma-Aldrich, product no. H0267) was dissolved in saline (or PBS) to a concentration of 2 mg/mL. Particles were suspended in saline (or PBS) and sonicated as previously described. Hemoglobin and particle solutions (final particle mass doses: 10, 50 and 100 μg/mL) were then exposed for 15 min at 37 °C followed by centrifugation for 5 min at 10,000 rpm. The concentration of hemoglobin in the supernatant was then analyzed from its change in absorbance at 540 nm as previously described for the hemolytic assay.

2.7. SEM analysis of nanoparticle–hemoglobin interactions

Ex situ analysis was performed to assess morphology changes of hemoglobin mixed with the particle suspensions by using a FEG-SEM instrument (LEO 1530 with Gemini column). Measurements were made at an operating voltage of 15 kV and an aperture size of 60 μm.

2.8. PCCS analysis of nanoparticle–hemoglobin interactions

Time-dependent particle size distribution measurements were conducted using photon cross correlation spectroscopy, PCCS (Nanophox, Sympatec GmbH) for particle suspensions in saline with and without hemoglobin (1 mg/mL). Nanoparticle-containing (1 mg/mL in saline) solutions (Cu, Cu-Zn or CuO) were ultrasonically treated for 3 min followed by particle size measurements after 0, 14 and 30 min, respectively. The importance of sonication using ultrasonic bath or ultrasonic tip compared with non-sonicated solutions was elucidated for Cu-nano in saline.

2.9. Particle interactions with model lipid membranes using QCM-D

1-palmitoyl-2-oleoyl-sn-glycero-3-phosphocholine (POPC), 1-palmitoyl-2-oleoyl-sn-glycero-3-phospho-L-serine (POPS) and 1-hexadecanoyl-2-(9Z-octadecenoyl)-sn-glycero-3-phospho-(1′-rac-glycerol) (POPG) were purchased from Avanti Polar Lipids Inc., USA, and used to prepare liposomes of mixed lipid composition (25% of POPS or POPG and 75% of POPC). The lipids were dissolved in chloroform and stored under N_2 at -20 °C. Liposomes (80–100 nm based on DLS measurements) were prepared as previously described (Kunze et al., 2009). QCM-D measurements were performed at several harmonics ($n = 3, 7, 13$) at 22 °C using a Q-Sense E4 instrument and 5 MHz SiO_2 coated quartz sensors (Q-Sense AB, Sweden). Frequency shifts were normalized to the fundamental frequency of the sensor by dividing the frequency shift with the overtone number of the resonant frequency. Data analysis was realized using the Q-Tools software (Q-Sense AB, Sweden). Prior to use, the sensors were exposed to UV/ozone for 30 min. Supported lipid membranes were formed *in situ* on the SiO_2 surfaces at a flow rate of 100 μL/min. Adsorption and spontaneous rupture of liposomes were achieved using 0.1 mg/mL liposome suspensions in PBS to which 5 mM $MgCl_2$ was added. Model membranes prepared in this way are characterized by frequency and dissipation shifts of -25 Hz and $< 0.5 \times 10^{-6}$, respectively (Keller and Kasemo, 1998). Suspensions of Cu, CuO and Cu-Zn nanoparticles in saline (mass doses of 0.1 and 0.3 mg/mL) were freshly prepared prior to the measurements as described above with the exception that sonication was performed using an ultrasonic bath (15 min) instead of a tip sonicator. Suspensions were injected as such in the QCM-D instrument at a flow rate of 50 or 100 μL/min. Despite the sonication treatment, dark agglomerates were sometimes visually observed.

3. Results

3.1. Particle characteristics

The measured surface area of dry powder particles (BET) decreased according to the following sequence: CuO » Cu > Cu-Zn » Cu micro (Table 1). TEM investigations were performed to examine the morphology and size of the Cu, Cu-Zn and CuO nanoparticles,

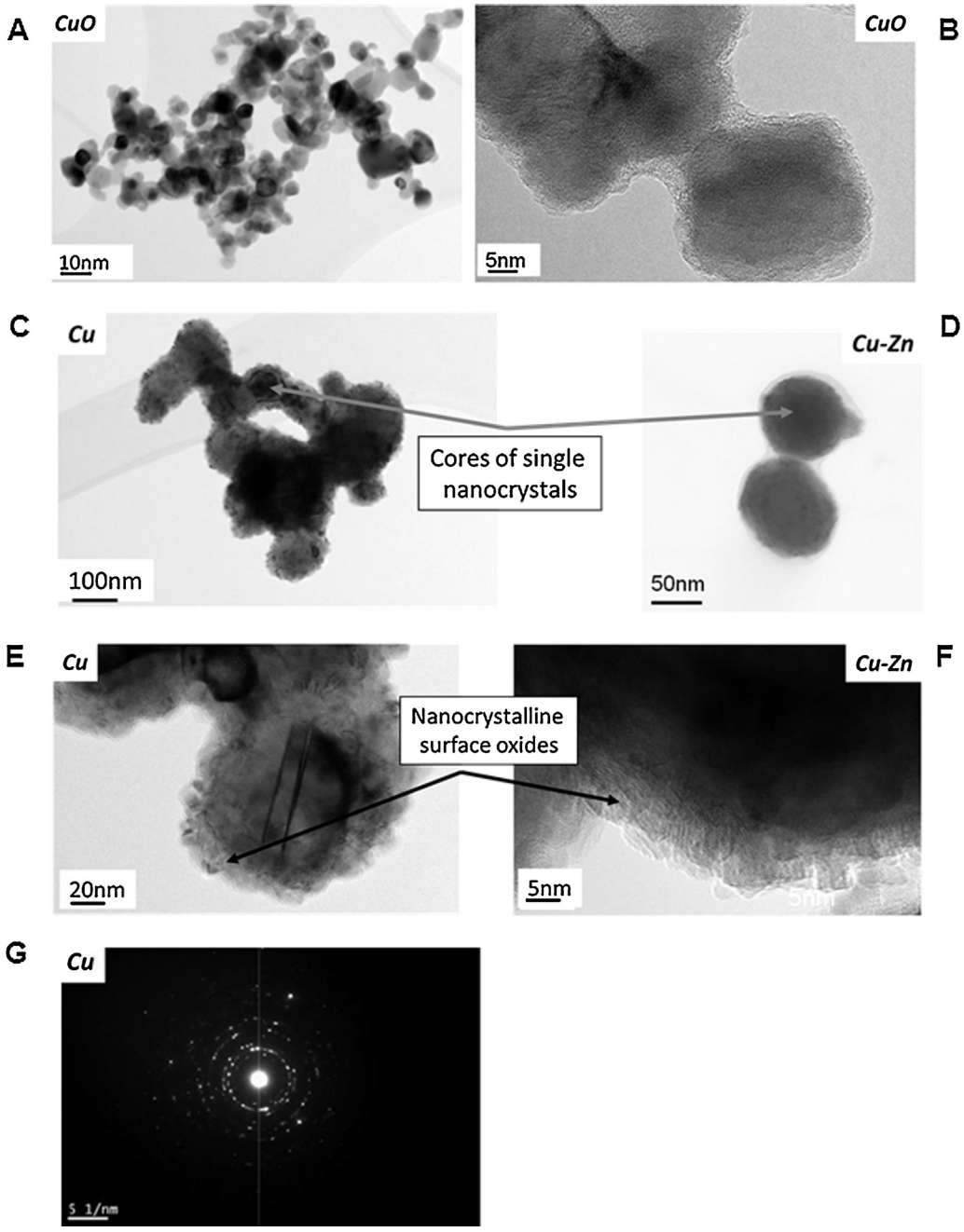

Fig. 1. TEM images (A-F) and electron diffraction pattern (G) of CuO nanoparticles (A-B), Cu nanoparticles (C, G), and Cu-Zn nanoparticles (D-F), measured by means of TEM (transmission electron microscopy, A-F) and EELS (electron energy-loss spectrometry, G).

combined with EELS and EDS measurements to assess their degree of crystallinity and surface oxide composition. The CuO nanoparticles formed large agglomerates of single particles, mean average size 50 nm, Fig. 1a-b. Their surface structure was however difficult to assess and the seemingly amorphous surface layer may be an artifact from the sample preparation. The Cu-nanoparticles predominantly consisted of large aggregates/agglomerates (Fig. 1c) of nano-sized primary particles (estimated mean size 100 nm)

Table 2
Released percentage of copper and zinc per added mass of particles incubated for 5 min in cell media (41965-039 from Invitrogen, contains mainly inorganic salts, amino acids, vitamins, glucose and 10% calf serum was added) or saline (0.9% NaCl, 154 mM).

	Release of Cu (% of particle mass)		Release of Zn (% of particle mass)	
Sample	Cell media	Saline	Cell media	Saline
Cu mico	0.23 ± 0.025	0.12 ± 0.018	–	–
Cu nano	8.5 ± 0.67	1.1 ± 0.59	–	–
Cu-Zn nano	5.0 ± 0.29	1.7 ± 0.18	8.1 ± 0.92	1.7 ± 0.094
CuO nano	3.6 ± 0.77	0.73 ± 0.50	–	–

– Not analyzed

with a crystalline surface oxide (Fig. 1e). Oxygen enrichment in the surface oxide was evident from EDS measurements and the crystalline nature of the surface oxide was further strengthened by the electron diffraction pattern showing clearly visible diffraction spots (Fig. 1g). The oxide thickness was approximately 5–20 nm. The presence of rings in the diffraction pattern is a consequence of different grain orientations (polycrystallinity). Few aggregates of single nanoparticles were observed without any observable surface oxide. Cu_2O and CuO were the main components of the outermost surface oxide of the Cu-nanoparticles in line with previous observations (Midander et al., 2009).

Nanoparticles of the binary Cu-Zn alloy were more dispersed and present in smaller agglomerates compared with Cu and CuO (Fig. 1f). Similar to the findings of Cu, these agglomerates consisted of single nano-sized particles (estimated mean size 75–100 nm) with a crystalline surface oxide. However, compared with Cu, this oxide was significantly thinner (approx. 5 nm) and composed of finer crystallites (compare Fig. 1c and d). The average particle composition by means of EELS revealed a Zn/(Zn + Cu) mass ratio of 0.48 ± 0.08, *i.e.* relatively consistent with the nominal bulk composition of the wire (0.40). Similar relative mass ratios were determined by means of EDS (0.40 ± 0.07). The main X-ray powder diffraction peaks of ZnO and possibly CuO were identified in addition to peaks related to Cu and Zn metal and to the brass alloy. According to XPS compositional findings, zinc-rich phases were predominant in the utmost surface layer as judged from a relative Zn/(Zn + Cu) mass ratio of 0.87. This is in agreement with literature findings showing that ZnO is the predominant oxide on Cu-Zn nanoparticles (Cokoja et al., 2006).

3.2. Particle characteristics in solution

Except from the characterization performed at dry conditions, particle size distribution in cell medium and PBS as well as zeta potential measurements (in 10 mM NaCl) were conducted. As reliable zeta potential measurements only are possible in media of low ionic strength (Kirby and Hasselbrink, 2004), no measurements were made in cell medium. PCCS analysis of particles in cell media showed different extent of particle agglomeration (Fig. 2). The metal particles formed agglomerates of different average sizes (by volume) with peaks at 200 and 650 nm for Cu nano (Fig. 2B), and peaks at 150 and 2000 nm for Cu-Zn nano (Fig. 2B). Agglomeration was also evident to some extent for CuO with agglomerates sized 300 nm (by volume) in addition to particles sized 20–90 nm (by volume) (Fig. 2C). The average size of proteins in cell media was determined to 4.6 nm (Fig. 2A).

Sonication changed the particle size distribution in solution (data not shown) but also the zeta potential. This effect was significant in the case of the Cu and Cu-Zn nano and was highly dependent on sonication strength. Stable measurements were only possible for sonicated particle suspensions except for CuO, which was possible to disperse in 10 mM NaCl without sonication due to its high zeta potential (repulsion forces) already at non-sonicated conditions (+27 mV). CuO showed a very high positive zeta potential, between +30 and +40 mV, independent of sonication strength. For Cu nano, the zeta potential increased upon sonication from near-neutral values at non-sonicated conditions to approximately +10 mV after sonication. Similar trends, although of slightly higher values were determined for Cu-Zn increasing from approximately +10 mV to +20 mV after sonication. From these observations follows an increased size distribution of the nano-sized particles in solution according to: CuO « Cu ≈ Cu-Zn.

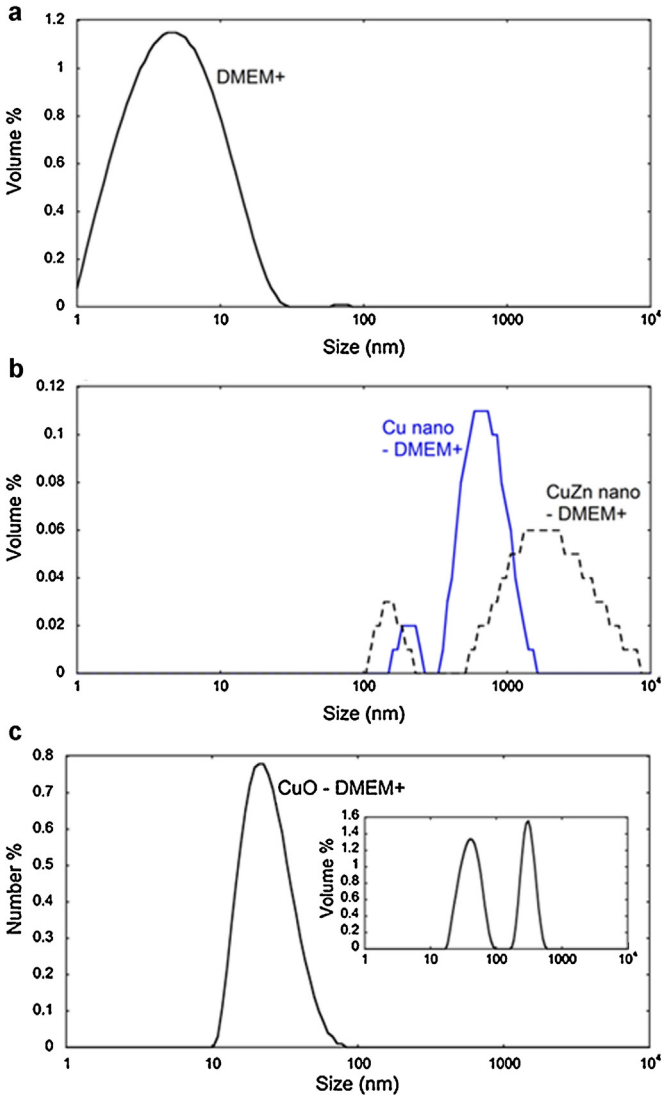

Fig. 2. Size distribution of DMEM medium supplemented with serum ($DMEM^+$) with or without particles measured by means of PCCS (photon cross correlation spectroscopy). The size distributions correspond to: (A) only DMEM media with serum (by volume %), (B) Cu and Cu-Zn nanoparticles (by volume %) and (C) CuO nanoparticles (by number % and by volume % in inset). The $DMEM^+$ size distribution is subtracted for clarity in B-C, meaning that the protein peak is not shown in B-C.

3.3. Metal release in cell media and saline

The extent of released metals in cell medium (pH approx. 7.4) from a given particle mass dose (40 μg/mL) was higher for Cu and Cu-Zn nanoparticles compared with CuO nano and Cu micro (Table 2). The amount of released copper and zinc from Cu-Zn showed a time-dependence with more zinc released compared to copper after 5 min, and *vice versa* after 4 h (Table 3). The particle mass was thus substantially reduced with time. After 4 h, only 21% (92% after 5 min) and 29% (87% after 5 min) of the particle mass remained for Cu and Cu-Zn, respectively. For Cu-Zn, almost 70% of the bulk content of both copper and zinc was released into solution after 4 h. The remaining mass of Cu micro exposed for 4 h in cell medium was 98% (99.8% after 5 min) and thus substantially higher compared with Cu nano. Particle exposure for 5 min in saline (relatively low ionic strength, pH approx. 6.5) resulted in a very low dissolution/metal ion release and thus only a small reduction of the particle mass, less than 4% for all particles for the particle mass dose investigated (100 μg/mL), see Table 2. These findings are in general

Table 3
Released percentage of copper and zinc per added mass of particles incubated for 4 h in cell media (41965-039 from Invitrogen, contains mainly inorganic salts, amino acids, vitamins, glucose and 10% calf serum was added).

Sample	Release of Cu (% of particle mass) Cell media	Release of Zn (% of particle mass) Cell media
Cu mico	2.0 ± 0.43	–
Cu nano	79 ± 0.29	–
Cu-Zn nano	42 ± 1.7	29 ± 1.5
CuO nano	29 ± 2.4	–

– Not analyzed

agreement with the literature (Gunawan et al., 2011). Similar to the observations in cell medium, the highest extent of released metals was observed for Cu-Zn and Cu followed by CuO and only minor amounts from Cu micro when suspended in saline. In contrast to the cell medium, similar concentrations of copper and zinc were released from Cu-Zn.

3.4. Membrane damage using trypan blue staining

When assessing the membrane integrity of lung cells exposed to a given particle mass (20 μg/mL) it was obvious that the Cu and Cu-Zn nanoparticles caused a rapid (within the first 4 h) increase in membrane damage, whereas CuO nano (largest surface area) and Cu micro showed no effect (Fig. 3a). Experiments were therefore performed where the cells were exposed to particle doses of a given dry surface area (based of BET). No large discrepancy in results between Cu nano and Cu micro was evident when the dose was expressed as surface area, see Fig. 3b (4 h) and 3c (18 h). Significantly higher levels of cell membrane damage were induced for Cu nano only for one dose (0.34 cm^2/cm^2) compared with the Cu micro, which consequently was exposed with a significantly higher particle mass (factor 67) compared with Cu nano. When comparing all particle types investigated in this study, it was evident that the Cu and Cu-Zn particles showed very similar effects up to a dose of 0.68 cm^2/cm^2 (Fig. 3b). However, the Cu-Zn particles caused a significantly higher extent of damage for the twofold dose, 1.36 cm^2/cm^2.

3.5. LDH assay interactions

Investigations of possible interactions with the LDH assay by mixing the particles with the reaction mix for the LDH assay clearly showed a pronounced increase in absorbance at 490 nm in the absence of LDH for Cu nano and Cu-Zn nano (Fig. 4). This change in absorbance indicates the presence of the LDH protein. CuO nanoparticles caused only a minor increase whereas micron-sized Cu caused no effect. The observed increase in absorbance was not related to absorbance due to the presence of particles since the particles suspended in saline without the reaction mix revealed no increase in absorbance (data not shown). The same test was performed in the presence of a known LDH concentration in order to investigate whether the particles affected the LDH protein (*e.g.* due to un-folding or absorbance of the protein to the particle surface). The results showed the same extent of increase in absorbance when compared with the control (LDH without particles) as the increase observed in the absence of LDH. This indicates that the interference is likely due to the fact that the particles catalyze the reaction producing red formazan rather than interacting with the LDH protein.

3.6. Hemolytic assay and hemoglobin interactions

Particle-cell membrane interactions were investigated using the hemolytic assay as a model. At the particle mass doses tested (up

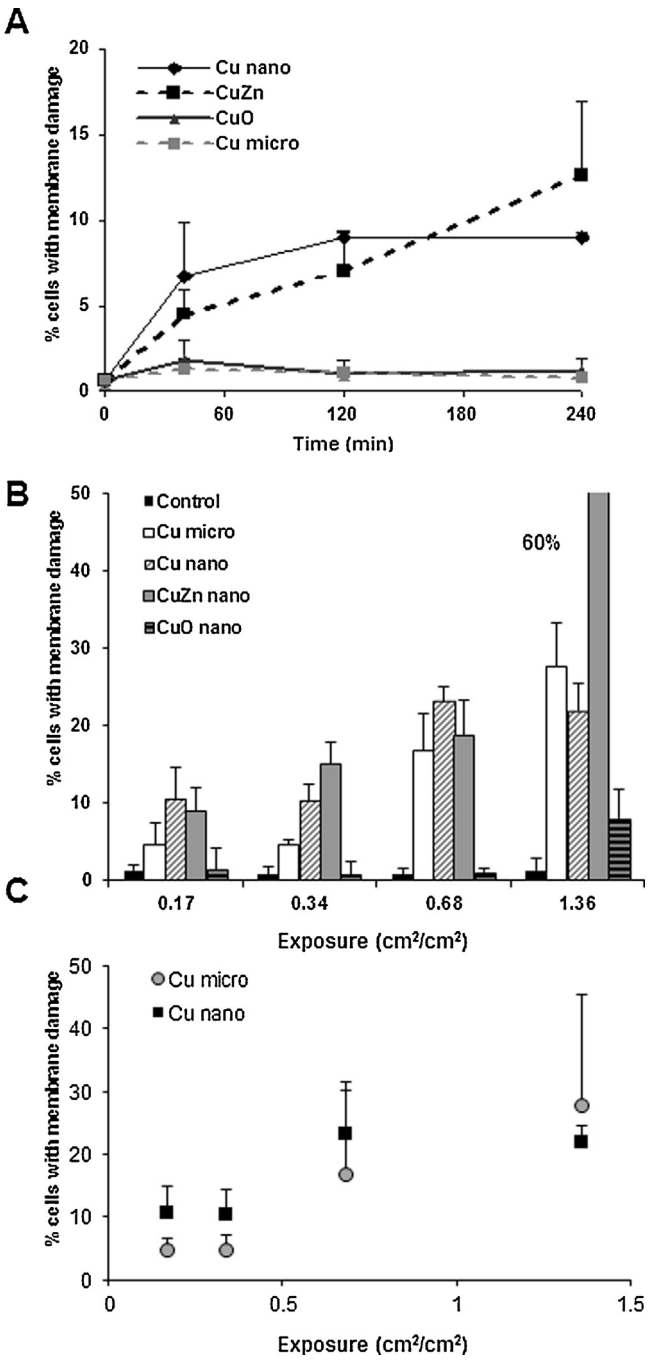

Fig. 3. Membrane damage analyzed using trypan blue staining after exposure of A549 cells to the different particles. In (A) cells were exposed to a particle mass dose of 20 μg/mL and membrane damage was assessed after 40 min, 2 h and 4 h. In (B) and (C) cells were exposed to the same surface area dose for 4 h (B) or 18 h (C).

to 1 mg/mL), only the positive control SiO_2 induced a release of hemoglobin, measured as an increase in absorbance at 540 nm (Fig. 5a). However, since both particles and released metal ionic species most probably interact with proteins, the interaction between the different particles and hemoglobin was investigated by mixing the particles with a hemoglobin solution of known concentration. Both Cu nano and Cu-Zn nano (100 μg/mL) almost completely cleared the hemoglobin from the solution (Fig. 5b). Dissolved copper from $CuCl_2$ (100 μg/mL) caused the same effect (see also Suppl. Fig. 2a). No studies were conducted using a water soluble zinc salt. Thus, in order to investigate whether the effect was a consequence of released metal ions, the influence on hemoglobin

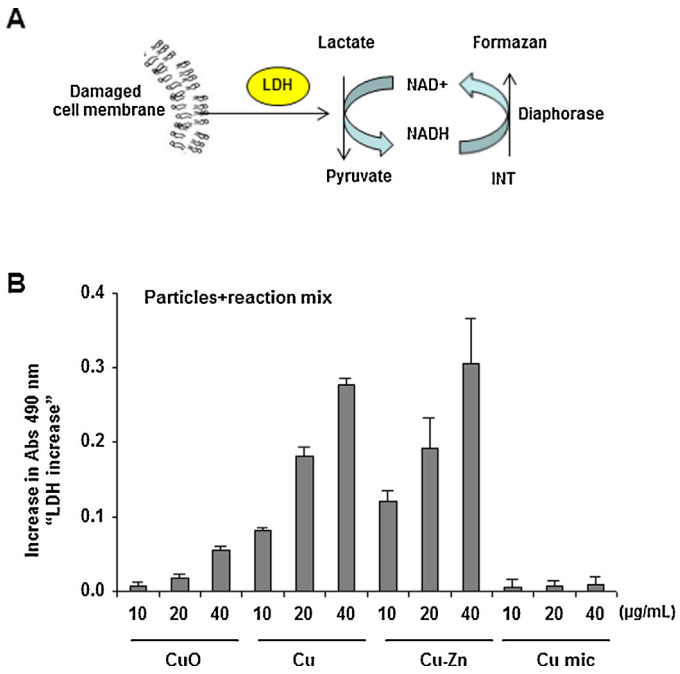

Fig. 4. Particle-LDH interactions. (A) Upon membrane damage the release of LDH (lactate dehydrogenase) is measured with a coupled enzymatic reaction that results in the conversion of a tetrazolium salt (iodonitrotetrazolium, INT) into formazan of red color that can be measured at an absorbance of 490 nm. (B) Cu and Cu-Zn nanoparticles catalyzed the conversion to formazan in the absence of LDH.

caused by the "released metal fraction" was investigated. This fraction is in this context defined as the supernatant collected after exposure of particle suspensions for 15 min at 37 °C followed by centrifugation (see experimental). Released ionic metal species in saline caused however only a minor effect. The same experiments performed in PBS instead of saline showed a different effect especially for Cu-Zn nano that in the presence of phosphate did not interact with hemoglobin (Suppl. Fig. 2b). In order to further test at what copper concentrations protein-interactions occur, a dose response test was performed for readily soluble $CuCl_2$ in saline in the concentration interval between 1 and 50 μg/mL. These experiments indicated that hemoglobin interaction started already at $CuCl_2$ concentrations of 1–5 μg/mL, *i.e.* approx. 0.5–2.5 μg/mL Cu, to be compared with approx. 1.5 μg/mL Cu in the released metal fraction from Cu nano upon exposure in saline for 5 min (Fig. 5c). Micron-sized Cu metal particles showed no hemoglobin-interactions, even when investigated at a similar dry surface area dose as Cu nano (data not shown).

3.7. SEM and PCCS analysis of nanoparticle–hemoglobin interactions

To further investigate the hemoglobin-nanoparticle interactions, precipitation/aggregation of hemoglobin in the presence of Cu and Cu-Zn nanoparticles was visualized by means of SEM. Fig. 6 clearly shows that Cu nano and Cu ionic species caused protein aggregation, whereas no effect was evident for CuO nano. PCCS measurements were employed to further confirm the depletion of hemoglobin from the solution. Size distributions measurements (by number %) of hemoglobin, with and without the addition of Cu-nano, are presented in Fig. 7. Observed data is in good agreement with the size of hemoglobin (approximately $5.4 \times 5.4 \times 19.4$ nm) with a peak between 1 and 27.6 nm (by volume) and between 1 and 12.2 nm (by number) with median diameters of 4.5 and 1.6 nm based on volume and number, respectively. The hemoglobin signal completely disappeared upon addition of Cu nano. This is in

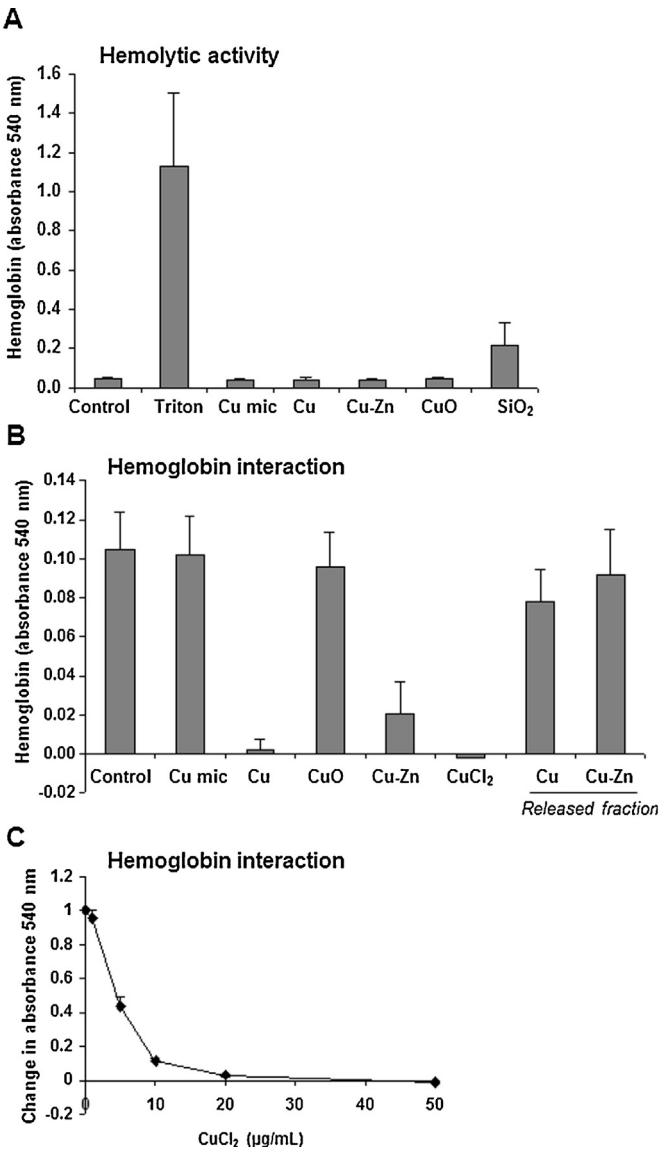

Fig. 5. Hemolytic activity and hemoglobin interaction. (A) Hemolytic activity was analyzed as released hemoglobin following exposure of the particles (1 mg/mL, 30 min at dark conditions and room temperature) with red blood cells derived from fresh venous blood from healthy blood donors. (B) Hemoglobin interactions were analyzed as the depletion of hemoglobin from a solution following exposure with particles (100 μg/mL, 15 min, 37 °C). In (C) hemoglobin was incubated with $CuCl_2$ and interactions were observed at concentrations 1–10 μg/mL corresponding to Cu concentrations of 0.5–5 μg/mL (the *y*-axis shows the relative change in absorbance compared to control without any $CuCl_2$).

agreement with the visual observation that the red color of the hemoglobin solution became grayish and then transparent after addition of Cu nano. To confirm that this phenomena not was general to all nanoparticles, additional tests were performed with Ag nanoparticles. When these nanoparticles were added to the hemoglobin solution, the red color remained and the hemoglobin peak was clearly visible at similar intensities compared with the hemoglobin solution without nanoparticles (data not shown).

3.8. Interactions with a model lipid membrane using QCM-D

Further nanoparticle-membrane interaction experiments were performed using a model membrane, supported on a sensor surface. Well-defined model membranes prepared on silica surfaces were exposed to the particle suspensions and the interactions

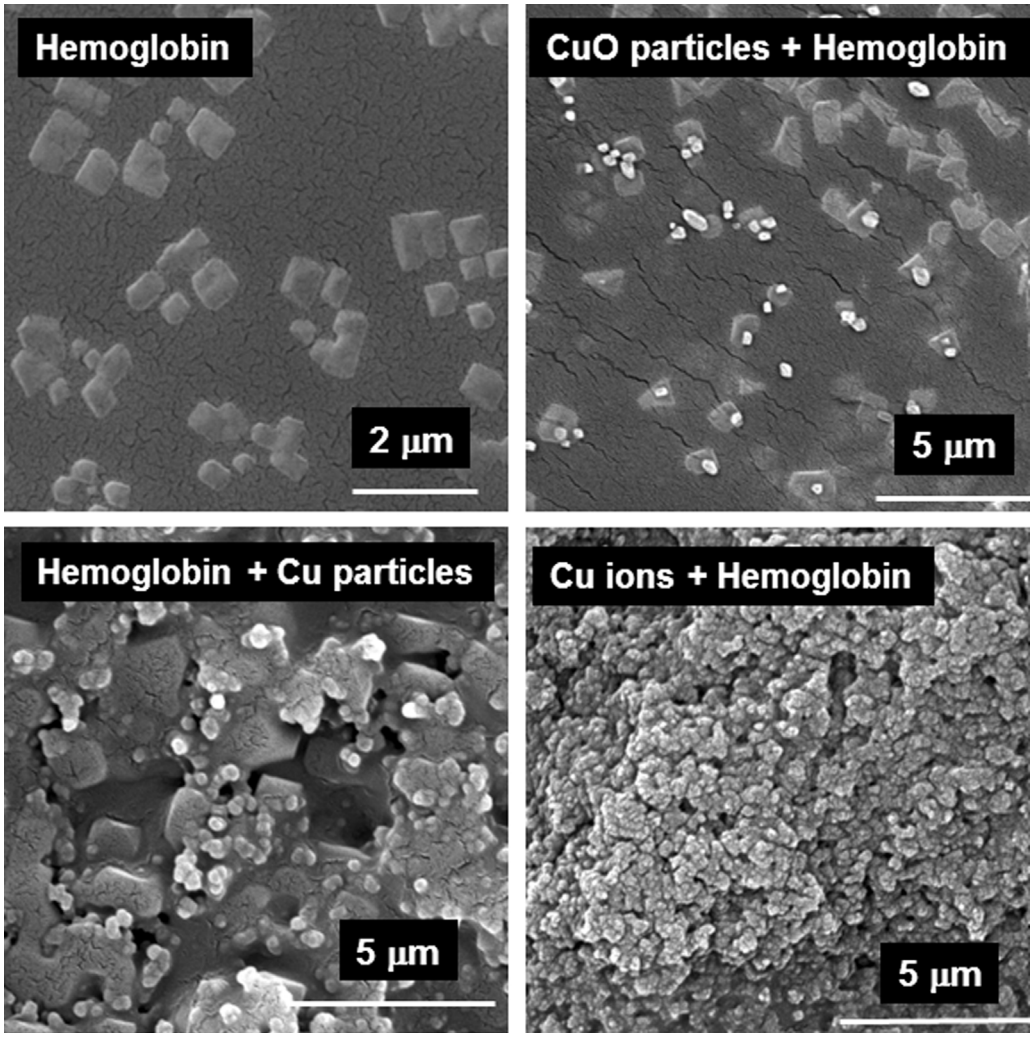

Fig. 6. SEM (scanning electron microscopy) images showing precipitation/aggregation of hemoglobin due to interaction with Cu nanoparticles and Cu ionic species, but not after interactions with CuO nanoparticles.

were recorded with QCM-D. QCM-D results obtained upon injection of Cu, CuO and Cu-Zn nanoparticles suspended in saline over model lipid membranes are presented in Fig. 8. Despite the relatively large variation between repeated experiments, most likely related to differences in particle size distribution and extent of agglomeration in the particle suspensions (see section 3.2), some differences were observed between the different particle suspensions with respect to their membrane interactions. Notably, small negative frequency shifts (corresponding to mass uptake) were observed upon injection of Cu-Zn nano, whereas small positive frequency shift (corresponding to mass removal) were observed upon injection of CuO nano (Fig. 8a). All particles gave rise to similar dissipation shifts (Fig. 8b), indicating a weak association of the particles with the membrane surface. The significantly increased dissipation shifts upon addition of the particles (Fig. 8b) corresponds to a change in the viscoelastic properties near the lipid membrane upon particle addition and consequently increased dissipative losses. This means that the structure is softer compared with the plain membrane (without any nanoparticle addition), probably due to a small number of particles deposited onto the membrane.

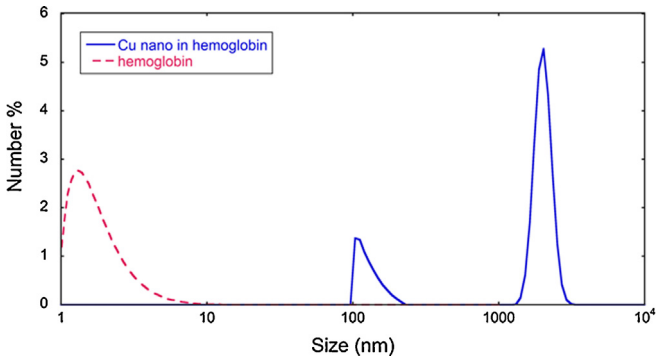

Fig. 7. Size distribution (by number %) of Cu nanoparticles in hemoglobin solution (solid line) and hemoglobin solution without any particles (dashed line), measured by means of PCCS (photon cross correlation spectroscopy). Note that the hemoglobin peak between 1 and 10 number % is absent upon Cu nanoparticle addition (solid line).

4. Discussion

In this study, we have shown a clear difference in reactivity toward cell membranes for nanoparticles of metallic Cu (with a surface oxide and a metallic core) and nanoparticles of cupric oxide CuO. CuO nano caused no or only minor effects on the cell membrane integrity, whereas the metallic Cu nanoparticles were significantly more reactive. Metallic Cu in micrometer size did not cause damage when cells were exposed to the same mass as the Cu nanoparticles. However, when the cells were exposed to the same

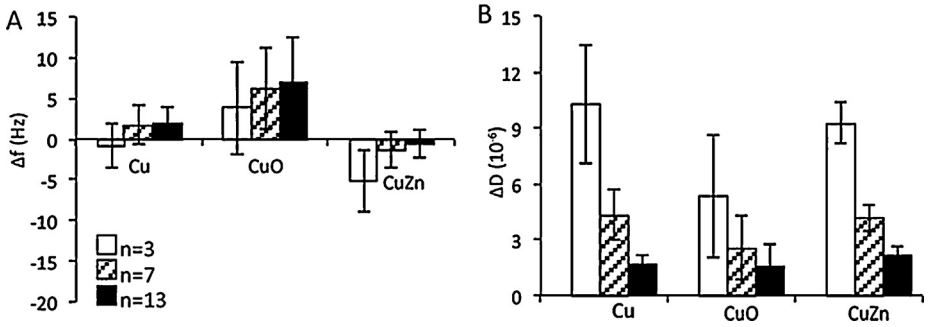

Fig. 8. QCM-D (quartz crystal microbalance – dissipation) measurements after particle interactions with model lipid membranes. Shift in frequency (A) and dissipation (B) are shown upon injection of Cu, CuO and Cu-Zn nanoparticles suspended in saline. Positive shifts in frequency correspond to a decrease in mass of the lipid membrane and positive shifts in dissipation indicate an increase in softness (viscoelastic properties) of the lipid membrane. $n = 3$, 7 and 13 are the different overtone (harmonic) numbers.

surface area (based on BET at dry conditions), the cell membrane damaging effect was more similar (Fig. 3b and c) implying that the effect, at least to some extent, seems to be related to the surface area. When exposed to the same surface area dose, the mass of the micron-sized Cu particles (Cu micro) was 67 times higher compared with Cu nanoparticles. This equals a very high mass dose of 1340 μg/mL at the surface area of dose of 0.68 cm^2/cm^2, to be compared with 20 μg/mL as the mass dose for the Cu nanoparticles. The surface area dose was based on the BET dry surface area. The actual surface in contact with the cell membrane will however be affected by particle agglomeration in the cell media and by the fact that the Cu nanoparticles release copper ions/dissolves with time with less and smaller particles that remain in the cell media as a consequence.

An important difference in the toxic response of Cu and CuO nanoparticles seems to be related to their different cellular targets. Previous findings by the authors have shown Cu nanoparticles on the cell surface, whereas none or very few particles were observed intracellulary (Cronholm et al., 2011). In contrast, CuO nanoparticles were observed within the cells after 4 h (Cronholm et al., 2013). These findings are in line with a study by Vanwinkle et al. (2009), in which no Cu nanoparticles were observed inside R3-1 cells, but only at the cell membrane surface. The dominant dissolution mechanism for Cu nano, Cu-Zn nano and Cu micro is most likely oxidation, *i.e.* corrosion. Based on redox equations, described in Vanwinkle et al. (2009), oxidation of Cu(s) to Cu^{2+} is energetically favorable along with a coupled production of H_2O_2 from oxygen and protons ($Cu\ (s) + O_2 + 2H^+ = Cu^{2+} + H_2O_2$). It is furthermore likely that the Cu nanoparticles are more easily oxidized when interacting with the cells since the cell membrane contains higher O_2 concentration when compared with the cell media. From this follows a local H_2O_2 production at the cell membrane and subsequent cell membrane damage (Vanwinkle et al., 2009). It is thus important to note that the cell membrane damage seems not to be directly caused by Cu ionic species but rather related to the actual *metal release process* taking place at the particle-cell surface interface. This is in agreement with previous studies by the authors that showed little damage to the cell membrane following exposure of A549 cells to dissolved Cu ionic species from a readily soluble Cu-compound (Cronholm et al., 2013; Karlsson et al., 2008). The importance of the metal release process taking place at the particle-cell surface interface is probably also important for Cu-Zn nano and is in line with literature findings reporting that the bacterial inhibitory ability of *e.g.* Cu- and Zn-based coatings is related to the amounts of H_2O_2 produced rather than effects observed for the respective ions (Zhao et al., 1998). This is also supported by a recent study showing high cell membrane damage caused by Cu nanoparticles, whereas no such effects were observed for carbon coated Cu nanoparticles and $CuCl_2$ (Minocha and Mumper, 2012).

The amount of released copper and zinc from Cu-Zn nano revealed a time-dependence with more zinc released compared with copper after 5 min, and *vice versa* after 4 h. This time-dependent dezincification process is consistent with literature findings for brass in aqueous media (Goidanich et al., 2011; Marshakov, 2002; Selvaraj et al., 2003). The Cu-Zn nanoparticles were by far the most membrane reactive when the particle dose was expressed based on dry surface area, an effect mainly observed for the highest dose. This is likely explained by a combination of H_2O_2 generation and toxicity induced by released zinc ionic species. This study thus highlights an unusually high toxicity of particles of a binary Cu-Zn (40% Zn) brass alloy, not very well studied before. Toxicity to *Daphnia magna* of brass particles has previously been shown (Johnson et al., 1986) as well as effects on pulmonary macrophages following exposure of rats to "brass dust" (30% Zn), (Anderson et al., 1988). Respiratory effects have been reported for workers who polish and produce brass-based utensils (30% Zn) in Sri Lanka (Jayawardana et al., 1997). Importantly, micrometer sized Cu-Zn particles (30% Zn) seem not to show as high toxicity (Karlsson et al., 2008b), possible due to less H_2O_2 production and less release of Cu and Zn ionic species.

In contrast to electrochemical dissolution (oxidation) occurring for the Cu and Cu-Zn nanoparticles, chemical dissolution (likely mainly ligand-induced) is the main dissolution mechanism for CuO. Importantly, chemical dissolution does not generate H_2O_2 as in the case of electrochemical dissolution and may thus at least partly explain observed differences. Findings on the dissolved mass percentage of CuO nanoparticles in cell media in this study are consistent with previous independent studies by the authors (Midander et al., 2009), but larger compared with *e.g.* a study by Studer et al. (2010). This is most likely explained by a higher mass dose (50-fold) of CuO nanoparticles and subsequent particle agglomeration in the study by Studer et al. Other studies report a lower extent of dissolution in different media such as distilled water (Xia et al., 2006), 5 g/L NaCl (Gunawan et al., 2011) and PBS (Midander et al., 2009). This highlights the importance of enhanced ligand-induced dissolution in the presence of inorganic ions, amino acids and proteins, present in the cell media.

Except from the trypan blue staining, this study aimed to use complementary methods for investigating cell membrane damage induced by the different Cu-based particles of this study. The LDH assay that investigates the release of LDH from the cells upon cell membrane damage was employed. However, this assay was found non-applicable for Cu-containing nanoparticles since the high reactivity of Cu nano and Cu-Zn nano resulted in interactions with the assay. The particles catalyzed the conversion of the tetrazolium salt into formazan (of red color) by diaphorase in the absence of LDH. The LDH activity can also be assessed in the absence of the coupled reaction used in the present study by analyzing the change in NADH levels. However, a recent study showed that Cu nanoparticles, as

well as copper ions, actually inactivate LDH making also this assay unsuitable for measuring toxicity of Cu (Han et al., 2011). Silver nanoparticles in a carbon matrix (used to entrap the particles during synthesis) caused the same effect, but not silver nanoparticles without this matrix. The nanoparticles can also interact by adsorbing LDH on the surface. This effect was observed for CuO nano in the present study, and was also evident for TiO_2 nanoparticles in the study by Han et al. (Han et al., 2011). These results highlight the importance of carefully evaluating possible nanoparticle-assay interactions within nanotoxicology research.

Due to their high membrane reactivity, Cu nano and Cu-Zn nano were expected to show hemolytic effects. However, none of the particles caused hemolysis of red blood cells, measured as released hemoglobin (Fig. 5a). However, since both nanoparticles caused hemoglobin aggregation/precipitation, any release of hemoglobin would have been precipitated and removed upon centrifugation together with the cells/cell debris and remaining particles. Hemoglobin aggregation/precipitation was confirmed using additional assays (Figs. 6 and 7). Aggregation of hemoglobin was not observed for Cu-Zn nano suspended in PBS instead of saline. This is most likely a consequence of differences in copper and/or zinc speciation in solution (as copper ions or zinc phosphates, c.f. discussion below), or possibly due to the formation of a protective phosphate layer on the particle surface reducing the reactivity as recently reported for ZnO nanoparticles (Lv et al., 2012). These results clearly elucidate how relatively small changes in experimental conditions (saline *vs.* PBS in this case) can dramatically influence the results. Cupric ions freshly dissolved from $CuCl_2$ in saline in concentrations similar to copper concentrations released from the Cu nanoparticles caused hemoglobin interactions. This indicates that the released ionic species could contribute to the aggregation of hemoglobin. On the other hand, studies with the released ionic fraction (separated from the particles) from Cu nano and Cu-Zn nano in saline did not show any substantial effects. The reason is believed to be attributed to the interaction of free copper and/or zinc ions released from the nanoparticles in the close vicinity of hemoglobin. The fraction of free copper and/or zinc ions (of the total released concentration) in solution is typically significantly lower as both ions rapidly form labile and strong complexes in aqueous solution. This formation is of significant importance in PBS (phosphates) or organic solutions (organic ligands). The effect of chloride (saline) and phosphate (PBS) on the speciation of copper and zinc is illustrated in Suppl. Figs. 3 and 4, exemplified for the measured released copper concentration in solution from Cu nano after 4 h in saline and PBS, respectively, and prevailing solution chemistry. Recently, Gunawan et al. (2011) showed that the released copper fraction from CuO nanoparticles was not as toxic as the same concentration of copper dissolved from a copper salt (copper nitrate or copper sulfate). Generated results were explained by differences in copper speciation in solution related to the formation of copper-peptide complexes (released fraction) and the presence of free copper ions (metal salts). The same study observed differences in how the pH of the solution decreased upon dissolution of a copper salt and was non-altered in the case with the released copper fraction (Gunawan et al., 2011). Precipitation of hemoglobin induced by the interaction of various metal ions has previously been reported. Compared with other metal ions, the copper(II)-ion was the most efficient ion able to precipitate hemoglobin closely followed by the zinc(II)-ion (Frantzen et al., 1997). Whereas zinc ions were rather specific toward hemoglobin, when compared to other serum proteins, copper ions were not specific and induced also hemoglobin oxidation (Frantzen et al., 1997). One study on the interactions between hemoglobin and Cu nanoparticles has previously been reported in the literature (Bhattacharya et al., 2006). Similar our study, Bhattacharya and coworkers reported precipitation of hemoglobin in the presence of Cu nanoparticles. They suggested a mechanism where hemoglobin unfolds (indicated by an increase in heme peroxidase activity) followed by misfolding-induced aggregation at higher concentrations (indicated by a reduction in peroxidase activity). No aggregation effects on non-heme proteins and a clear difference among different types of hemoglobin (HbA0, HbA2, HbE) were reported.

Nanoparticle–lipid membrane interactions were further investigated using model lipid membranes supported to a sensor surface and a corresponding surface sensitive analytical technique (here QCM-D). Significantly increased dissipation shifts confirmed particle-membrane interactions, but no significant differences were observed between the different nanoparticles investigated. Obtained results in frequency shift (indicating a mass change) showed relatively high variation, most likely due to particle agglomeration, but support in general the findings of the different responses among the nanoparticles of this study. A higher mass loss for the more membrane reactive particles (Cu and Cu-Zn) was initially expected but instead the CuO nanoparticles caused a slight mass loss. This is likely a consequence of lipid adsorption on the particles that results in a mass loss of the membrane. A recent study by some of the authors showed that protein adsorption could not be recorded by means of QCM-D for a copper surface due to its rapid dissolution (Lundin et al., 2012). Future studies using lipid bilayers will include investigations of model membranes containing polyunsaturated lipids as these are prone to be affected by lipid peroxidation.

5. Conclusion

In conclusion, cell membrane damage caused by different Cu-containing nanoparticles (Cu metal, Cu-Zn alloy, CuO) depends both on chemical composition (metal *vs.* oxide) and surface area. Furthermore, nanoparticles of Cu and Cu-Zn seem to have an ability to precipitate proteins such as hemoglobin, effects not observed for nanoparticles of CuO or micron-sized Cu particles. Generated results suggest that the metal release process of Cu nano and Cu-Zn nano taking place at the cell membrane surface is responsible for the observed membrane damage. This process is predominantly governed by electrochemical (oxidative) dissolution that results in a local generation of H_2O_2, a process not taking place for CuO. These results highlight the difference in reactivity and thus toxicity between metallic Cu nanoparticles (with an oxide surface) and CuO nanoparticles, differences that may be important for read across possibilities. The present study also highlights that assay interactions indeed are important to consider in the field of nanotoxicology.

Conflict of interest

None.

Acknowledgment

This study was financially supported by the Swedish Research Council (VR), the Swedish Council for Working Life and Social Research (FAS project 2011-0832), and Cusanuswerk, Germany (Yolanda Hedberg), and FORMAS (NanoSphere project). Help with PCCS from Dr. Jonas Hedberg and Dr. Troy Lowe, Div. Surface and Corrosion Science, is highly appreciated as well as valuable discussions with Assoc. Prof. Eva Blomberg, Div. Surface and Corrosion Science. We also thank Dr. Anna Godymchuk, University of Tomsk, for providing the Cu and Cu-Zn nanoparticles. M.Sc. Rodrigo Robinson, Institute for Surface Chemistry, is highly acknowledged for performing the SEM investigation of hemoglobin-particle interactions.

Appendix A. Supplementary data

Supplementary data associated with this article can be found, in the online version, at http://dx.doi.org/10.1016/j.tox.2013.07.012.

References

Ahamed, M., Siddiqui, M.A., Akhtar, M.J., Ahmad, I., Pant, A.B., Alhadlaq, H.A., 2010. Genotoxic potential of copper oxide nanoparticles in human lung epithelial cells. Biochem. Biophys. Res. Commun. 396, 578–583.

Allaker, R.P., 2010. The use of nanoparticles to control oral biofilm formation. J. Dent. Res. 89, 1175–1186.

Anderson, R.S., Gutshall, L.L., Thomson, S.A., 1988. Responses of rat alveolar macrophages to inhaled brass powder. J. Appl. Toxicol. 8, 389–393.

Bhattacharya, J., Choudhuri, U., Siwach, O., Sen, P., Dasgupta, A.K., 2006. Interaction of hemoglobin and copper nanoparticles: implications in hemoglobinopathy. Nanomedicine 2, 191–199.

Chen, Z., Meng, H., Xing, G., Chen, C., Zhao, Y., Jia, G., Wang, T., Yuan, H., Ye, C., Zhao, F., Chai, Z., Zhu, C., Fang, X., Ma, B., Wan, L., 2006. Acute toxicological effects of copper nanoparticles in vivo. Toxicol. Lett. 163, 109–120.

Cokoja, M., Parala, H., Schröter, M.K., Birkner, A., van der Berg, M.W.E., Klementiev, K.V., Grunert, W., Fischer, R.A., 2006. Nano-brass colloids: synthesis by co-hydrogenolysisof [CpCu(PMe_3)] with [ZnCp*2] and investigation of the oxidation behavior of a/b-CuZn nanoparticles. J. Mater. Chem. 16, 2420–2428.

Cronholm, P., Midander, K., Karlsson, H.L., Elihn, K., Odnevall Wallinder, I., Möller, L., 2011. Effect of sonication and serum proteins on copper release from copper nanoparticles and the toxicity towards lung epithelial cells. Nanotoxicology 5, 269–281.

Cronholm, P., Karlsson, H.L., Hedberg, J., Lowe, T., Winnberg, L., Elihn, K., Odnevall Wallinder, I., Möller, L., 2013. Intracellular uptake and toxicity of Ag- and CuO-nanoparticles–a comparison between nanoparticles and their corresponding metal ion. Small 9, 970–982.

Frantzen, F., Grimsrud, K., Heggli, D.E., Sundrehagen, E., 1997. Selective precipitation of human hemoglobin by organic solvents and metal cations. Hemoglobin 21, 155–172.

Goidanich, S., Brunk, J., Herting, G., Arenas, M.A., Odnevall Wallinder, I., 2011. Atmospheric corrosion of brass in outdoor applications: patina evolution, metal release and aesthetic appearance at urban exposure conditions. Sci. Total Environ. 15, 412–413.

Gunawan, C., Teoh, W.Y., Marquis, C.P., Amal, R., 2011. Cytotoxic origin of copper(II) oxide nanoparticles: comparative studies with micron-sized particles, leachate, and metal salts. ACS Nano 5, 7214–7225.

Han, X., Gelein, R., Corson, N., Wade-Mercer, P., Jiang, J., Biswas, P., Finkelstein, J.N., Elder, A., Oberdörster, G., 2011. Validation of an LDH assay for assessing nanoparticle toxicity. Toxicology 287, 99–104.

Hanagata, N., Zhuang, F., Connolly, S., Li, J., Ogawa, N., Xu, M., 2011. Molecular responses of human lung epithelial cells to the toxicity of copper oxide nanoparticles inferred from whole genome expression analysis. ASC Nano 5 (12), 9326–9338.

Hedberg, Y., Gustafsson, J., Karlsson, H.L., Möller, L., Odnevall Wallinder, I., 2010. Bioaccessibility, bioavailability and toxicity of commercially relevant iron- and chromium-based particles: in vitro studies with an inhalation perspective. Part. Fibre. Toxicol. 7, 23.

Jayawardana, P.L., de Alwis, W.R., Fernando, M.A., 1997. Ventilatory function in brass workers of Gadaladeniya, Sri Lanka. Occup Med (Lond) 47, 411–416.

Johnson, D.W., Haley, M.V., Hart, G.S., Muse, W.T., Landis, W.G., 1986. Acute toxicity of brass particles to *Daphnia magna*. J. Appl. Toxicol. 6, 225–228.

Karlsson, H.L., Cronholm, P., Gustafsson, J., Möller, L., 2008. Copper oxide nanoparticles are highly toxic: a comparison between metal oxide nanoparticles and carbon nanotubes. Chem. Res. Toxicol. 21, 1726–1732.

Karlsson, H.L., Holgersson, A., Möller, L., 2008b. Mechanisms related to the genotoxicity of particles in the subway and from other sources. Chem. Res. Toxicol. 21, 726–731.

Karlsson, H.L., Gustafsson, J., Cronholm, P., Möller, L., 2009. Size-dependent toxicity of metal oxide particles-a comparison between nano- and micrometer size. Toxicol. Lett. 188, 112–118.

Kasemets, K., Ivask, A., Dubourguier, H.C., Karhu, A., 2009. Toxicity of nanoparticles of ZnO, CuO and TiO_2 to yeast Saccharomyces cerevisiae. Toxicol In Vitro 23, 1116–1122.

Keller, C.A., Kasemo, B., 1998. Surface specific kinetics of lipid vesicle adsorption measured with a quartz crystal microbalance. Biophys. J. 75, 1397–1402.

Kirby, B.J., Hasselbrink, E.F., 2004. Zeta potential of microfluidic substrates: 1. Theory, experimental techniques, and effects on separations. Electrophoresis. 25, 187–202.

Kunze, A., Svedhem, S., Kasemo, B., 2009. Lipid transfer between charged supported lipid bilayers and oppositely charged vesicles. Langmuir 25, 5146–5158.

Kwon, Y.S., Ilyin, A.P., Nazarenko, O.B., Tikhonov, D.V., 2008. Characteristics of nanopowders produced by electrical explosion of copper wires in argon with air additives. The Third International Forum on Strategic Technologies, IFOST 2008.

Lanone, S., Rogerieux, F., Geys, J., Dupont, A., Maillot-Marechal, E., Boczkowski, J., Lacroix, G., Hoet, P., 2009. Comparative toxicity of 24 manufactured nanoparticles in human alveolar epithelial and macrophage cell lines. Part. Fibre Toxicol. 30, 6: 14.

Lin, Y.S., Haynes, C.L., 2010. Impacts of mesoporous silica nanoparticle size, pore ordering, and pore integrity on hemolytic activity. J. Am. Chem. Soc. 132, 4834–4842.

Lu, S., Duffin, R., Poland, C., Daly, P., Murphy, F., Drost, E., Macnee, W., Stone, V., Donaldson, K., 2009. Efficacy of simple short-term in vitro assays for predicting the potential of metal oxide nanoparticles to cause pulmonary inflammation. Environ. Health Perspect. 117, 241–247.

Luechinger, N.A., Athanassiou, E.K., Stark, W.J., 2008. Graphene-stabilized copper nanoparticles as an air-stable substitute for silver and gold in low-cost ink-jet printable electronics. Nanotechnology 19, 445201.

Lundin, M., Hedberg, Y., Jiang, T., Herting, G., Wang, X., Thormann, E., Blomberg, E., Odnevall Wallinder, I., 2012. Adsorption and protein-induced metal release from chromium metal and stainless steel. J. Colloid Interface Sci. 366, 155–164.

Lv, J., Zhang, S., Luo, L., Han, W., Zhang, J., Yang, K., Christie, P., 2012. Dissolution and microstructural transformation of ZnO nanoparticles under the influence of phosphate. Environ. Sci. Technol. 46, 7215–7221.

Marshakov, I.K., 2002. Anodic dissolution and selective corrosion of alloys. Prot. Met. 38, 118–123.

Midander, K., Cronholm, P., Karlsson, H.L., Elihn, K., Möller, L., Leygraf, C., Odnevall Wallinder, I., 2009. Surface characteristics, copper release, and toxicity of nano- and micrometer-sized copper and copper(II) oxide particles: a cross-disciplinary study. Small 5, 389–399.

Minocha, S., Mumper, R.J., 2012. Effect of carbon coating on the physico-chemical properties and toxicity of copper and nickel nanoparticles. Small 8, 3289–3299.

Pham, L.Q., Sohn, J.H., Kim, C.W., Park, J.H., Kang, H.S., Lee, B.C., Kang, Y.S., 2012. Copper nanoparticles incorporated with conducting polymer: effects of copper concentration and surfactants on the stability and conductivity. J. Colloid Interface Sci. 365, 103–109.

Ren, G., Hu, D., Cheng, E.W., Vargas-Reus, M.A., Reip, P., Allaker, R.P., 2009. Characterisation of copper oxide nanoparticles for antimicrobial applications. Int. J. Antimicrob. Agents 33, 587–590.

Roduner, E., 2006. Size matters: why nanomaterials are different. Chem. Soc. Rev. 35, 583–592.

Saterlie, M., Sahin, H., Kavlicoglu, B., Liu, Y., Graeve, O., 2011. Particle size effects in the thermal conductivity enhancement of copper-based nanofluids. Nanoscale Res. Lett 6, 217.

Selvaraj, S., Ponmariappan, S., Natesan, M., Palaniswamy, N., 2003. Dezincification of brass and its control–an overview. Corros. Rev. 21, 41–74.

Shi, J., Hedberg, Y., Lundin, M., Odnevall Wallinder, I., Karlsson, H.L., Möller, L., 2012. Hemolytic properties of synthetic nano- and porous silica particles: the effect of surface properties and the protection by the plasma corona. Acta Biomater. 8, 3478–3490.

Studer, A.M., Limbach, L.K., Van Duc, L., Krumeich, F., Athanassiou, E.K., Gerber, L.C., Moch, H., Stark, W.J., 2010. Nanoparticle cytotoxicity depends on intracellular solubility: comparison of stabilized copper metal and degradable copper oxide nanoparticles. Toxicol. Lett. 197, 169–174.

Sun, T., Yan, Y., Zhao, Y., GuO, F., Jiang, C., 2012. Copper oxide nanoparticles induce autophagic cell death in A549 cells. PLos One 7 (8).

Torres, A., Ruales, C., Pulgarin, C., Aimable, A., Bowen, P., Sarria, V., Kiwi, J., 2010. Innovative high-surface-area CuO pretreated cotton effective in bacterial inactivation under visible light. ACS Appl. Mater. Interfaces 2, 2547–2552.

Vanwinkle, B.A., de Mesy Bentley, K.L., Malecki, J.M., Gunter, K.K., Evans, I.M., Elder, A., Finkelstein, J.N., Oberdörster, G., Gunter, T.E., 2009. Nanoparticle (NP) uptake by type I alveolar epithelial cells and their oxidant stress response. Nanotoxicology 3, 307–318.

Wang, Z., Li, N., Zhao, J., White, J.C., Qu, P., Xing, B., 2012. CuO nanoparticle interaction with human epithelial cells: cellular uptake, location, export, and genotoxicity. Chem. Res. Toxicol. 25, 1512–1521.

Zhao, Z.H., Sakagami, Y., Osaka, T., 1998. Toxicity of hydrogen peroxide produced by electroplated coatings to pathogenic bacteria. Can. J. Microbiol. 44, 441–447.

Xia, X., Xie, C., Cai, S., Yang, Z., Yang, X., 2006. Corrosion characteristics of copper microparticles and copper nanoparticles in distilled water. Corros. Sci. 48, 3924–3932.